



Study of curcumin and genistein interactions with human serum albumin

Jean-Sébastien Mandeville, Emilie Froehlich, H.A. Tajmir-Riahi*

Département de Chimie-Biologie, Université du Québec à Trois-Rivières, C. P. 500, Trois-Rivières, Québec G9A 5H7, Canada

ARTICLE INFO

Article history:

Received 24 October 2008

Received in revised form

27 November 2008

Accepted 28 November 2008

Available online 3 December 2008

Keywords:

Drug

HSA

Binding

Conformation

Spectroscopy

ABSTRACT

Curcumin, the yellow pigment from the rhizoma of *Curcuma longa*, is a widely studied polyphenolic compound which has a variety of biological activity as anti-inflammatory and antioxidative agent. Genistein one of the flavonoids found in soybean and chickpeas inhibits DNA strand breaks acting as a direct scavenger of reactive oxygen species. Human serum albumin (HSA) with high affinity binding sites is a major transporter for delivering several endogenous compounds and drugs *in vivo*. The aim of this study was to examine the interactions of curcumin and genistein with human serum albumin at physiological conditions, using constant protein concentration and various pigment contents. FTIR, UV–Visible, CD and fluorescence spectroscopic methods were used to analyse drug binding mode, the binding constant and the effects of pigment complexation on HSA stability and conformation. Structural analysis showed that curcumin and genistein bind HSA *via* polypeptide polar groups with overall binding constants of $K_{\text{curcumin}} = 5.5 (\pm 0.8) \times 10^4 \text{ M}^{-1}$ and $K_{\text{genistein}} = 2.4 (\pm 0.40) \times 10^4 \text{ M}^{-1}$. The number of bound pigment (n) is 1.33 for curcumin and 1.49 for genistein. The HSA conformation was altered by pigment complexation with reduction of α -helix and increase of random coil and turn structures suggesting a partial protein unfolding.

© 2009 Elsevier B.V. All rights reserved.

1. Introduction

Curcumin 1,7-bis-(4-hydroxy-3-methoxyphenyl)-1,6-heptadiens-3,5-dione (Scheme 1) the main yellow pigment of the powdered rhizome (turmeric) of the herb *Curcuma longa* has been used for centuries as a spice and food coloring agent [1]. It has also been used to treat diseases such as inflammation, skin wounds and tumors as traditional medicine [2]. Curcumin exhibits antioxidant activity both *in vivo* and *in vitro* [1]. Apart from its anti-inflammatory, antimicrobial and antiviral properties curcumin is considered as cancer chemopreventive agent [3,4]. Mechanisms by which curcumin prevent cancer were attributed to several effects including anti-angiogenic action, up-regulation of enzymes detoxifying carcinogens and inhibition of certain signal transduction pathways for tumor cell growth and neutralization of carcinogenic free radicals [1,2]. Curcumin–protein interactions have been studied and the effect of curcumin on inhibition and activation of protein kinase C is reported [5].

Genistein 4',5,7-trihydroxy isoflavone (Scheme 1) presents in soybean and chick peas has a wide spectrum of physiological and pharmacological functions. It is known to antagonize human melanoma cell growth at G2/M transition [6] and found to inhibit

$\text{H}_2\text{O}_2/\text{Cu(II)}$ mediated DNA strand breaks acting as a direct scavenger of reactive oxygen species with the OH group at C-4 position responsible for its antioxidant activity [7]. Genistein intercalation into DNA and RNA duplexes is known [8–10] and the effects of genistein on activation of protein phosphatases is well investigated [11].

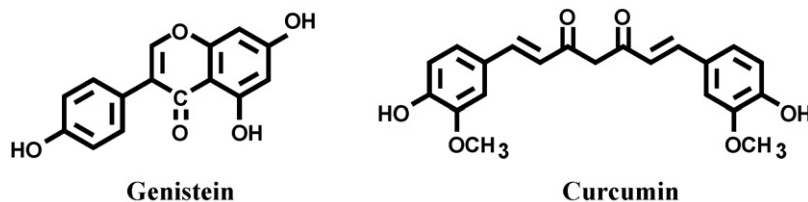
Human serum albumin (Scheme 2) is the most abundant serum protein, which carries several endogenous compounds including fatty acids. HSA has long been the center of attention of pharmaceutical industry due to its ability to bind various drug molecules and alters their pharmacokinetic properties [12]. HSA is a globular protein composed of three structurally similar domains (I, II and III), each containing two subdomains (A and B) and stabilized by 17 disulphide bridges [13–20]. Aromatic and heterocyclic ligands were found to bind within two hydrophobic pockets in subdomains IIA and IIIA, namely site I and site II [13–20]. Seven binding sites for fatty acids are localized in subdomains IB, IIIA, IIIB and on the subdomain interfaces [13]. HSA has also a high affinity metal binding site at the N-terminus [14]. These multiple binding sites underline the exceptional ability of HSA to interact with many organic and inorganic molecules and make this protein an important regulator of intercellular fluxes, as well as the pharmacokinetic behaviour of many drugs [13–21]. Therefore, it was of interest to study the binding of curcumin and genistein on protein secondary structure, conformation and stability.

In this report, the spectroscopic analysis of HSA complexation with curcumin and genistein was carried out in aqueous solution at physiological conditions, using constant protein concentration and

Abbreviations: HAS, human serum albumin; cur, curcumin; gen, genistein; FTIR, Fourier transform infrared spectroscopy; CD, circular dichroism.

* Corresponding author. Tel.: +1 819 376 5011x3310; fax: +1 819 376 5084.

E-mail address: tajmirri@uqtr.ca (H.A. Tajmir-Riahi).



Scheme 1. Chemical structures of genistein and curcumin.

various pigment contents. Structural information regarding pigment binding mode and the effects of complexation on the protein stability and secondary structure is reported here.

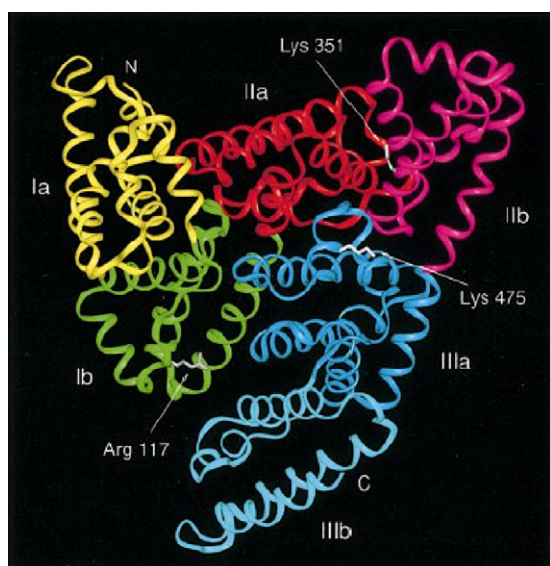
2. Experimental

2.1. Materials

HSA fraction V and curcumin and genistein were purchased from Sigma Chemical Company (St-Louis, MO) and used as supplied. Other chemicals were of reagent grade and used without further purification.

2.2. Preparation of stock solutions

Human serum albumin was dissolved in aqueous solution (40 mg/ml or 0.5 mM) containing 10 mM Tris-HCl buffer (pH 7.4). The protein concentration was determined spectrophotometrically using the extinction coefficient of $36,500 \text{ M}^{-1} \text{ cm}^{-1}$ at 280 nm [22]. In this study, HSA did not have its fatty acids removed, in a way to reproduce normal physiological conditions, where between 0.1 and 2 fatty acid molecules are bound to albumin [14–21]. Curcumin or genistein 2 mM was first prepared in water/ethanol 50% and then diluted to 0.125, 0.25, 0.5 and 1 mM in water/ethanol 50%. After addition of equal volume (0.2 ml) of pigment solution to (0.2 ml) of protein solution, the drug concentrations of 0.125, 0.25, 0.5 and 1 mM were reached and the final ethanol concentration was reduced to 25%. The presence of ethanol 25% induces no major HSA structural changes according to a recent publication [23].



Scheme 2. Human serum albumin.

2.3. FTIR spectroscopic measurements

Infrared spectra were recorded on a FTIR spectrometer (Impact 420 model), equipped with deuterated triglycine sulphate (DTGS) detector and KBr beam splitter, using AgBr windows. Solution of pigment was added dropwise to the protein solution with constant stirring to ensure the formation of homogeneous solution and to reach drug concentrations of 0.125, 0.25, 0.5 and 1 mM with a final protein concentration of 0.25 mM (20 mg/ml). Spectra were collected after 2 h incubation of HSA with pigment solution at room temperature, using hydrated films. Interferograms were accumulated over the spectral range $4000\text{--}600 \text{ cm}^{-1}$ with a nominal resolution of 4 cm^{-1} and 100 scans. The difference spectra [(protein solution + pigment solution) – (protein solution)] were generated using the polypeptide antisymmetric and symmetric C–H stretching bands [24], located at $2900\text{--}2800 \text{ cm}^{-1}$, as internal standard. These bands, which are due to protein C–H stretching vibrations, do not undergo any spectral changes (shifting or intensity variation) upon pigment complexation and therefore, they are commonly used as internal standard. When producing difference spectra these bands were adjusted to the baseline level, in order to normalize difference spectra. Details regarding infrared spectral treatment are given in our recent publication [25].

2.4. Analysis of protein secondary structure

Analysis of the secondary structure of HSA and its pigment complexes was carried out on the basis of the procedure previously reported [26]. The protein secondary structure is determined from the shape of the amide I band, located around $1660\text{--}1650 \text{ cm}^{-1}$. The FT-IR spectra were smoothed and their baselines were corrected automatically using Grams AI software. Thus the root-mean square (rms) noise of every spectrum was calculated. By means of the second derivative in the spectral region $1700\text{--}1600 \text{ cm}^{-1}$ seven major peaks for HSA and the complexes were resolved. The above spectral region was deconvoluted by the curve-fitting method with the Levenberg-Marquadt algorithm and the peaks corresponds to α -helix ($1658\text{--}1655 \text{ cm}^{-1}$), β -sheet ($1638\text{--}1614 \text{ cm}^{-1}$), turn ($1677\text{--}1660 \text{ cm}^{-1}$), random coil ($1648\text{--}1640 \text{ cm}^{-1}$) and β -antiparallel ($1692\text{--}1680 \text{ cm}^{-1}$) were adjusted and the area was measured with the Gaussian function. The area of all the component bands assigned to a given conformation were then summed up and divided by the total area [27]. The curve-fitting analysis was performed using the GRAMS/AI Version 7.01 software of the Galactic Industries Corporation.

2.5. Circular dichroism

CD Spectra of HSA and its pigment complexes were recorded with a Jasco J-720 spectropolarimeter. For measurements in the far-UV region (178–260 nm), a quartz cell with a path length of 0.01 cm was used in nitrogen atmosphere. HSA concentration was kept constant ($12.5 \mu\text{M}$), while varying each pigment concentrations (0.125,

Table 1
Secondary structure analysis (infrared spectra) from the free HSA and its pigment complexes in hydrated film at pH 7.4.

| Amide I component (cm ⁻¹) | Free HSA (%) 0.25 mM | Curcumin–HSA (%) 1 mM | Genistein–HSA (%) 1 mM |
|---------------------------------------|----------------------|-----------------------|------------------------|
| 1692–1680 β-anti | 7 | 4 | 4 |
| 1680–1660 turn | 14 | 15 | 18 |
| 1660–1650 α-helix | 55 | 51 | 48 |
| 1648–1641 random coil | 7 | 16 | 17 |
| 1640–1610 β-sheet | 17 | 14 | 12 |

0.25, 0.5 and 1 mM). An accumulation of three scans with a scan speed of 50 nm per minute was performed and data were collected for each nm from 260 to 180 nm. Sample temperature was maintained at 25 °C using a Neslab RTE-111 circulating water bath connected to the water-jacketed quartz cuvettes. Spectra were corrected for buffer signal and conversion to the Mol CD ($\Delta\epsilon$) was performed with the Jasco Standard Analysis software. The protein secondary structure was calculated using CDSSTR, which calculates the different assignments of secondary structures by comparison with CD spectra, measured from different proteins for which high quality X-ray diffraction data are available [28,29]. The program CDSSTR is provided in CDPro software package which is available at the website: <http://lamar.colostate.edu/~sreeram/CDPro>.

2.6. Absorption spectroscopy

The absorption spectra were recorded on a PerkinElmer Lambda 40 Spectrophotometer. Quartz cuvettes of 1 cm were used for determination of protein concentration.

2.7. Fluorescence spectroscopy

Fluorometric experiments were carried out on a Varian Cary Eclipse. Stock solutions of pigment 1 mM in ethanol/water were prepared at room temperature (24 ± 1 °C). Various solutions of pigment (10–400 μM) were prepared from the above stock solutions by successive dilutions also at 24 ± 1 °C. Solution of HSA (15 μM)

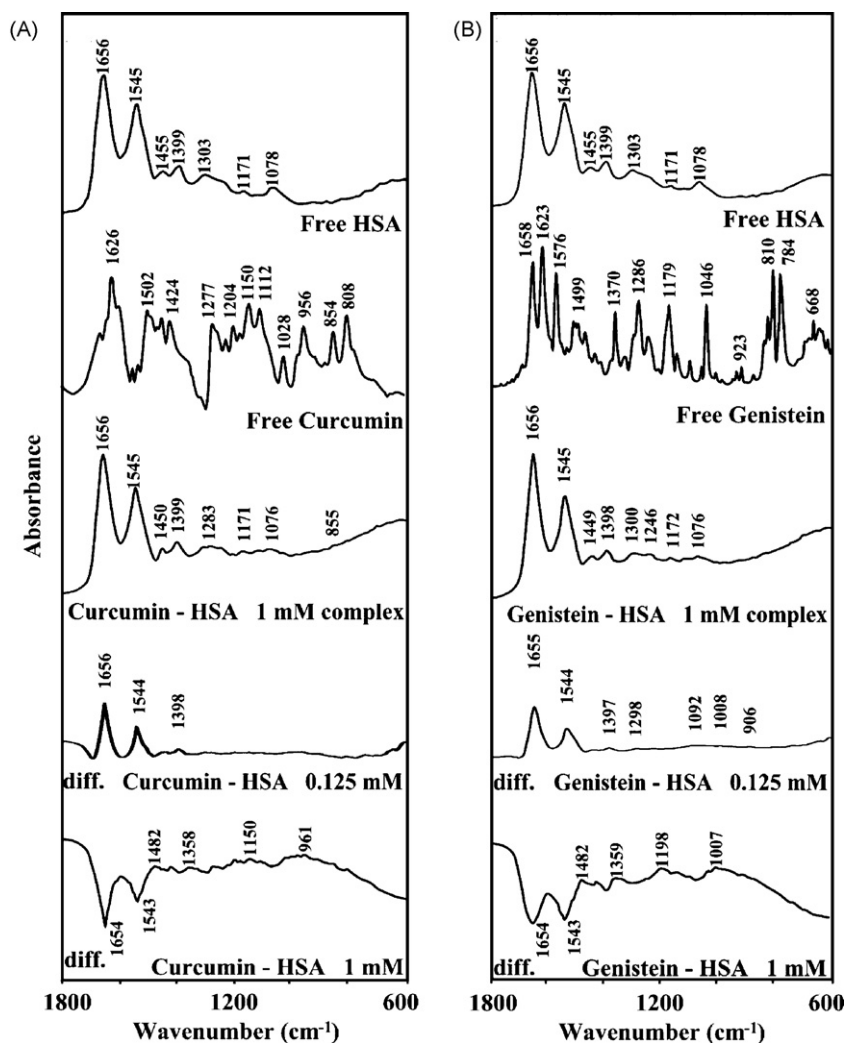


Fig. 1. (A) FTIR spectra in the region of 1800–600 cm⁻¹ of hydrated films (pH 7.4) for free HSA (0.25 mM), free curcumin (1 mM) and curcumin–HSA (1 mM) (top three curves) and difference spectra (diff.) of curcumin–HSA complexes (bottom two curves) obtained at different pigment concentrations (indicated on the figure) and (B) FTIR spectra in the region of 1800–600 cm⁻¹ of hydrated films (pH 7.4) for free HSA (0.25 mM), free genistein (1 mM) and genistein–HSA (1 mM) (top three curves) and difference spectra (diff.) of genistein–HSA complexes (bottom two curves) obtained at different pigment concentrations (indicated on the figure).

Table 2

Secondary structure of HSA complexes (CD spectra) with pigment at pH 7.4 calculated by CDSSTR software.

| Compound | α -helix (%) | β -sheet (%) | Turn (%) | Random (%) |
|----------------------|---------------------|--------------------|----------|------------|
| Free HSA | 58 | 9 | 11 | 22 |
| Curcumin–HSA (1 mM) | 54 | 10 | 12 | 24 |
| Genistein–HSA (1 mM) | 52 | 11 | 13 | 24 |

in 10 mM Tris–HCl (pH. 7.4) was also prepared at $24 \pm 1^\circ\text{C}$. The above solutions were kept in the dark and used soon after. Samples containing 0.4 ml of the above HSA solution and 0.4 ml of various pigment solutions were mixed to obtain final pigment concentration of 5–200 μM with constant HSA content 7.5 μM . The fluorescence spectra were recorded at $\lambda_{\text{exc}} = 280 \text{ nm}$ and λ_{em} from 287 to 500 nm. The intensity at 337 nm (tryptophane) was used to calculate the binding constant (K) according to previous literature reports [30–32].

3. Results and discussion

3.1. FTIR spectra of curcumin- and genistein–HSA complexes

The pigment–HSA interaction was characterized by infrared spectroscopy and its derivative methods. Since there was no major spectral shifting for the protein amide I band at 1656 cm^{-1} (mainly C=O stretch) and amide II band at 1544 cm^{-1} (C–N stretching coupled with N–H bending modes) [24–26] upon pigment interaction, the difference spectra [(protein solution + pigment solution) – (protein solution)] were obtained, in order to monitor the intensity variations of these vibrations and the results are shown in Fig. 1. Similarly, the infrared self-deconvolution with second derivative resolution enhancement and curve-fitting procedures [25] were used to determine the protein secondary structures in the presence of pigments (Fig. 2 and Table 1). CD spectroscopy was also used to analyse the protein conformation in the pigment–HSA complexes and the results are shown in Fig. 3 and Table 2.

At low pigment concentration (0.125 mM), intensity increase was observed for the protein amide I at 1656 cm^{-1} and amide II at 1545 cm^{-1} , in the difference spectra of the curcumin- and genistein–HSA complexes (Fig. 1, diff., 0.125 mM). Positive features are located in the difference spectra for amide I and II bands at 1656 , 1544 cm^{-1} (curcumin) and 1655 , 1544 cm^{-1} (genistein) (Fig. 1, diff., 0.125 mM). These positive features are related to increase in the intensity of the amide I and amide II bands upon pigment complexation. The increase in intensity of the amide I and amide II bands is due to pigment binding to protein C=O, C=N and N–H groups. Additional evidence to support the pigment interactions with C–N and NH groups comes from the shifting of the protein amide A band at 3296 cm^{-1} (N–H stretching mode) in the free HSA to 3298 (curcumin) and 3293 cm^{-1} (genistein), upon pigment complexation.

As pigment concentration increased to 0.5 and 1 mM, strong negative features for amide I were observed at 1654 and 1543 cm^{-1} for both curcumin and genistein in the difference spectra of pigment–HSA complexes (Fig. 1, diff., 1 mM). The observed decrease in intensity of the amide I band at 1656 cm^{-1} in the spectra of the polymer–protein complexes suggests a major reduction of protein α -helical structure at high pigment concentrations. Similar infrared spectral changes observed for protein amide I band in several drug–HSA complexes, where major protein conformational changes occurred [33].

A quantitative analysis of the protein secondary structure for the free HSA and its polymer adducts in hydrated films has been carried out and the results are shown in Fig. 3 and Table 1. The free protein has 55% α -helix (1657 cm^{-1}), β -sheet 17% (1616 , 1625

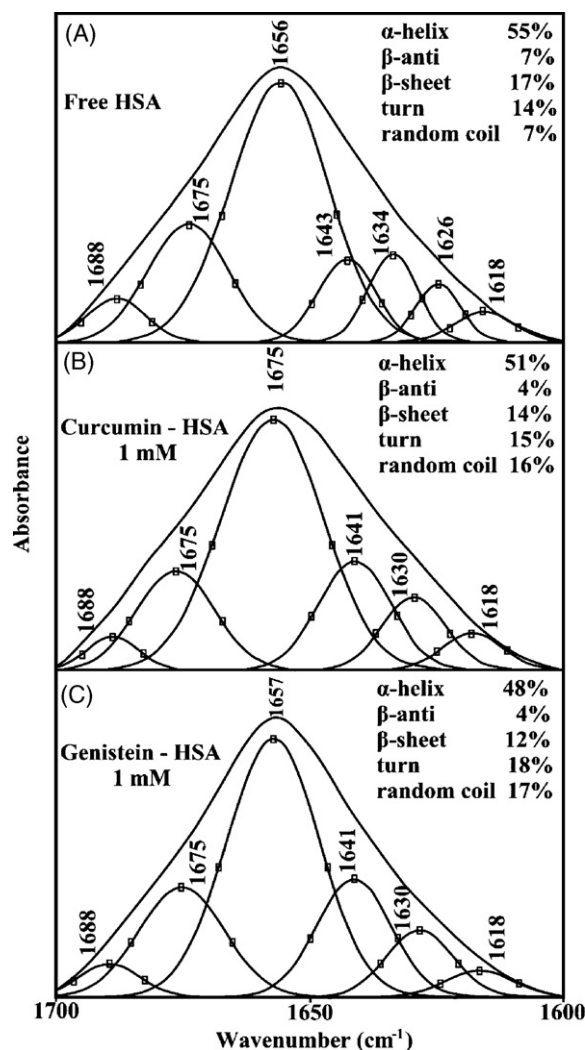


Fig. 2. Second derivative resolution enhancement and curve-fitted amide I region ($1700\text{--}1600 \text{ cm}^{-1}$) for free HSA (A) and its curcumin (B) and genistein (C) adducts in aqueous solution with 1 mM pigment and 0.25 mM protein concentrations at pH 7.4.

and 1634 cm^{-1}), turn structure 14% (1677 cm^{-1}), β -antiparallel 7% (1688 cm^{-1}) and random coil 7% (1643 cm^{-1}) (Fig. 2A and Table 1). The β -sheet structure is composed of three components at 1616 (inter β -strand), 1625 (intra β -strand) and 1634 cm^{-1} (hydrated) that are consistent with the spectroscopic studies of human serum albumin [34–38]. Upon pigment interaction, a major decrease of α -helix from 55% (free HSA) to 51% (curcumin–HSA) and 48% (genistein–HSA) with an increase in random coil from 7% (free HSA) to 16% (curcumin–HSA) and 17% (genistein–HSA) and minor increase of turn structure from 14% (free HSA) to 15% (curcumin–HSA) and 18% (genistein–HSA) (Fig. 3 and Table 1). The decrease in α -helix structure and increase in random coil and turn structure suggest a partial protein unfolding high pigment concentration.

3.2. CD spectra

The CD spectroscopic results shown in Fig. 3 and Table 2 exhibit marked similarities with those of the infrared data. Secondary structures calculations based on CD data suggests that free HSA has a high α -helix content 58%, β -sheet 9%, turn, 11% and random coil 22% (Fig. 3 and Table 2) which is consistent with the literature report [39]. Upon pigment complexation, reduction of α -helix

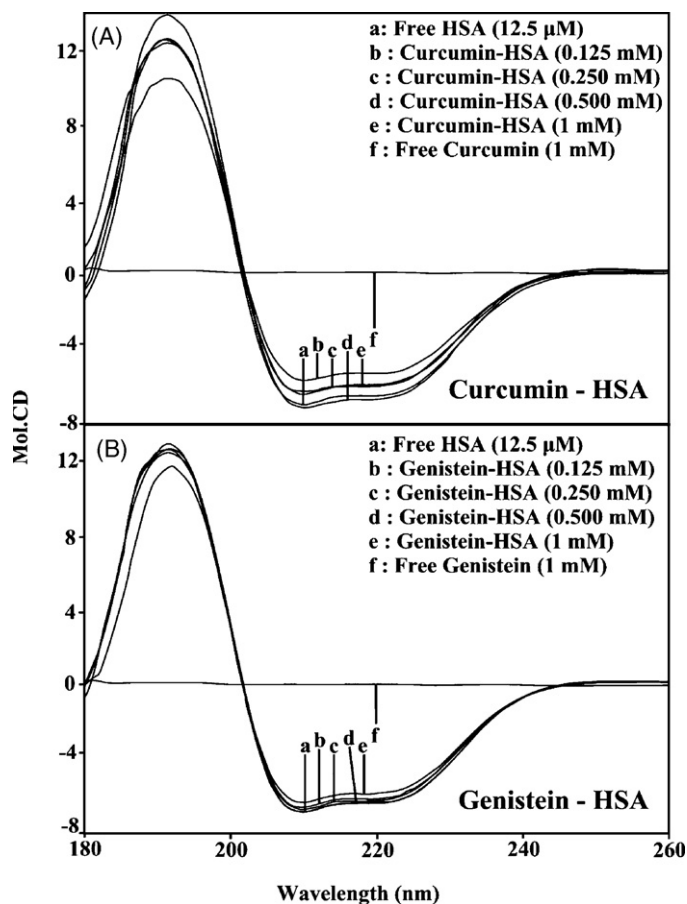


Fig. 3. Circular dichroism of free HSA and its pigment complexes in aqueous solution with protein concentration of 12.5 μM and pigment concentrations of 0.125, 0.25, 0.5 and 1 mM in 10 mM Tris-HCl buffer pH 7.4, 25% ethanol at 25 $^{\circ}\text{C}$.

was observed from 58% free HSA to 54% curcumin-HSA and 52% genistein-HSA complexes (Fig. 3 and Table 2). The minor decrease in alpha-helix was accompanied by an increase in the random coil and turn structure (Table 2). The reduction of the α -helix with an increase in the random coil and turn structure are consistent with the infrared results that showed reduction of alpha-helix and increase of random coil structure (Tables 1 and 2), indicating of some degree of protein unfolding upon pigment complexation. It should be noted that there are minor differences between IR vs CD results regarding free HSA conformation (Tables 1 and 2). The reason for the differences may be due to sample preparation since IR measurements were performed in hydrated films, whereas CD experiments were conducted in aqueous solutions.

3.3. Fluorescence spectra and binding constants of pigment-HSA complexes

HSA contains a single polypeptide of 585 amino acids with only one tryptophan (Trp 214) located in subdomain II A. Tryptophan 214 emission dominates HSA fluorescence spectra in the UV region. When other molecules interact with HSA, tryptophan fluorescence may change depending on the impact of such interaction on the protein conformation, or *via* direct quenching effect. On the assumption that there are (n) substantive binding sites for quencher (Q) on protein (B), the quenching reaction can be shown as following.



The binding constant (K_A), can be calculated as:

$$K_A = \frac{[Q_nB]}{[Q]^n[B]} \quad (2)$$

where $[Q]$ and $[B]$ are the quencher and protein concentration, respectively, $[Q_nB]$ is the concentration of non fluorescent fluorophore-quencher complex.

$$[Q_nB] = [B_0] - [B] \quad (3)$$

$$K_A = \frac{[B_0] - [B]}{[Q]^n[B]} \quad (4)$$

The fluorescence intensity is proportional to the protein concentration as describe:

$$\frac{[B]}{[B_0]} \propto \frac{F}{F_0} \quad (5)$$

Results from fluorescence measurements can be used to estimate the binding constant of lipid-protein complex. From Eq. (4):

$$\log \left[\frac{(F_0 - F)}{F} \right] = \log K_A + n \log [Q] \quad (6)$$

where F_0 is initial fluorescence intensity and F is fluorescence intensities in the presence of quenching agent (or interacting molecule). K is the Stern-Volmer quenching constant, $[Q]$ is the molar concentration of quencher and f is the fraction of accessible fluorophore to a polar quencher, which indicates the fractional fluorescence contribution of the total emission for an interaction with a hydrophobic quencher [40–43]. The plot of $F_0/(F_0 - F)$ vs $1/[Q]$ yields f^{-1} as the

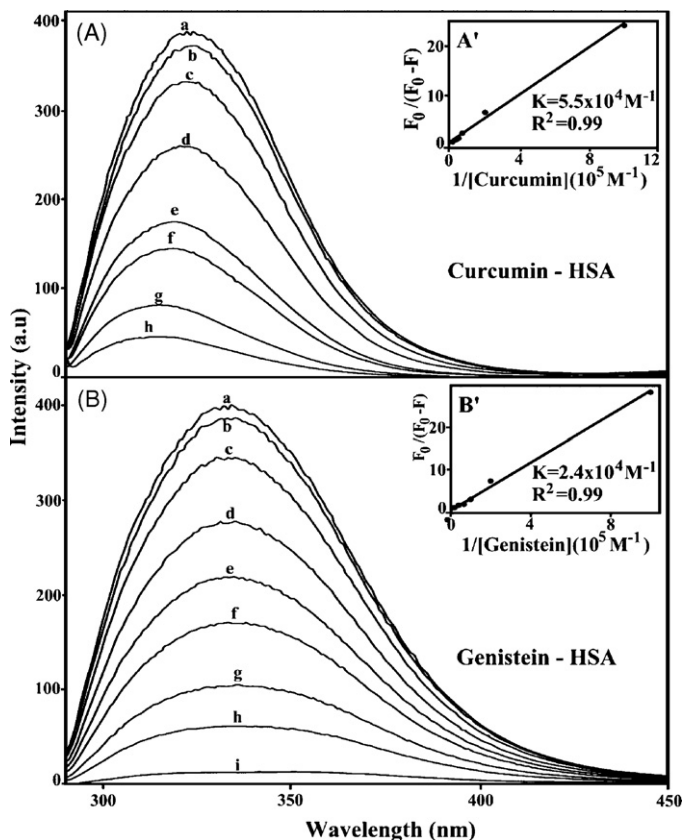


Fig. 4. Fluorescence emission spectra of pigment-HSA systems in 10 mM Tris-HCl buffer pH 7.4, 25% ethanol at 25 $^{\circ}\text{C}$ for A) curcumin-HSA; (a) free HSA, (b–g) HSA 7.5 μM with curcumin at 1, 5, 15, 25, 35, 50, 100 μM B) genistein-HSA; (a) free HSA (7.5 μM), (b–g) HSA 7.5 μM with genistein at 1, 5, 10, 15, 25, 37, 50, 100 μM (no absorption band for free genistein and curcumin in this region). The plot of $F_0/(F_0 - F)$ as a function of $1/\text{pigment concentration}$. The binding constant K being the ratio of the intercept and the slope for (A') curcumin-HSA and (B') genistein-HSA complexes.

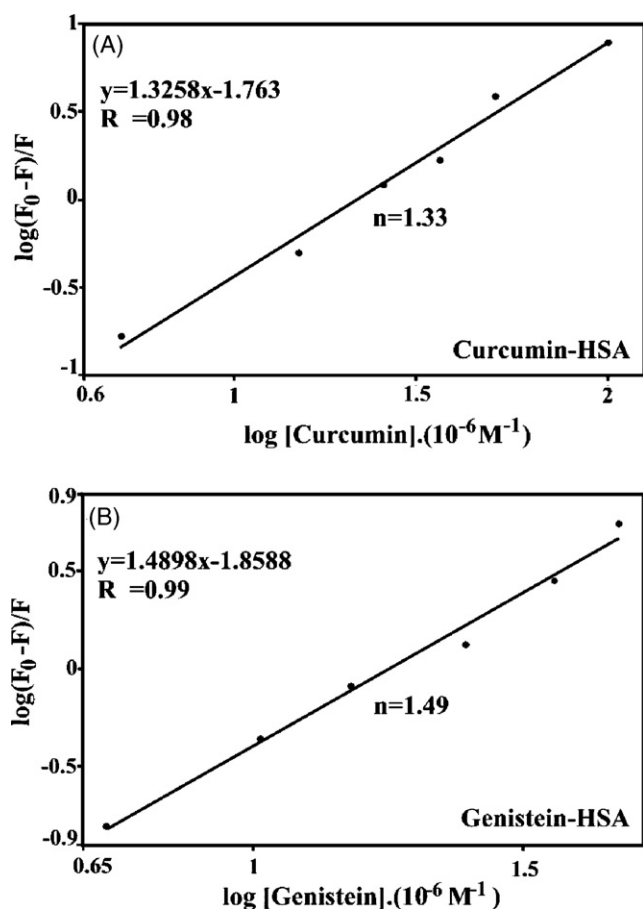


Fig. 5. The plot of $\log(F_0 - F)/F$ as a function of $\log[\text{pigment}]$ for calculation of number of binding (n) for curcumin-HSA (A) and genistein-HSA (B) complexes.

intercept on y axis and $(fK)^{-1}$ as the slope. Thus, the ratio of the ordinate and the slope gives K . The decrease of fluorescence intensity of HSA has been monitored at 330 nm for HAS–pigment systems (Fig. 4 shows representative results for each system). The plot of $F_0/(F_0 - F)$ vs $1/[\text{pigment}]$ (Fig. 4A and B show representative plots). Assuming that the observed changes in fluorescence come from the interaction between pigment and HSA, the quenching constant can be taken as the binding constant of the complex formation. The K values given here are averages of five replicate runs for HSA/pigment systems, each run involving several different concentrations of polyphenols (Fig. 4A' and B'). The binding constants obtained were $K_{\text{curcumin}} = 5.5 \times 10^4 \text{ M}^{-1}$ and $K_{\text{genistein}} = 2.4 \times 10^4 \text{ M}^{-1}$ (Fig. 4A' and B'). The association constants calculated for the pigment–HSA suggest low affinity polyphenol–HSA binding, compared to the other strong ligand–protein complexes with binding constants ranging from 10^6 to 10^8 M^{-1} [12,44]. However, lower binding constants (10^4 – 10^5 M^{-1}) were recently reported for several other ligand–protein complexes using fluorescence spectroscopic methods [30–33,42–43], consistent with our results.

The f values shown in Fig. 4 suggest that pigment interact with fluorophore *via* hydrophobic interactions too. As a result, we predict that the only fluorophore Trp 214 is relatively buried inside the HSA. This argument is based on the fact that the emission λ_{max} of Trp 214 was 330 nm (Fig. 4A and B), which is the emission region of hidden tryptophan molecules known to be usually around 320–325 nm [42–43], while fluorescence emission of exposed tryptophan molecule is around 340 nm due to solvent relaxation. The tightening of protein structure through intramolecular interactions, such as hydrogen bonds seems to bury Trp 214 in a more hydrophobic environment. The change in fluorescence intensity of Trp 214 in

the presence of pigment may arise as a direct quenching or as a result of conformational changes induced after pigment binding to HSA. The results indicate that pigment interaction do not change the emission λ_{max} at 330 nm. No spectral shift was observed for the emission spectra upon pigment–HSA complexation, indicating that Trp 214 was not exposed to any change in polarity. The emission λ_{max} of quenched tryptophan remains at 330 nm suggesting that pigment may interact with HSA *via* hydrophobic region located inside the protein. Based on molecular modeling and docking study, recent reports on pigment–protein interaction showed the locations of curcumin [45] and genistein [46] in the vicinity of Trp 214, consistent with our spectroscopic results.

The number of ligand bound (n) can be calculated from $\log[(F_0 - F)/F] = \log K_S + n \log[\text{pigment}]$ for the static quenching [47–51]. The linear plot of $\log[(F_0 - F)/F]$ as a function of $\log[\text{pigment}]$ shown in Fig. 5. The n values from the slope of the straight line are 1.33 for curcumin and 1.49 for genistein–HSA complexes (Fig. 5). The larger binding observed for genistein ($n = 1.49$) is consistent with more perturbations of HSA secondary structure inducing protein unfolding (Tables 1 and 2).

Even though curcumin and genistein are structurally different, they have similar hydrophobic affinity toward HSA binding and therefore both are mainly bound in the hydrophobic pockets of Trp 214 in the site I of IIA domain. The similar binding modes of the two drugs causes almost similar effects on the protein secondary structure as we shown in Tables 1 and 2 and Figs. 1–3. However, hydrophilic interaction with pigment OH groups can be also established in other protein binding domains.

4. Summary

Based on our spectroscopic results curcumin and genistein bind human serum albumin *via* both hydrophilic and hydrophobic interactions with stronger affinity for curcumin than genistein. However, larger binding of genistein induces more perturbations of HSA secondary structure with a partial protein unfolding. The pigment binding site is mainly in the subdomain II A (site I), where tryptophan 214 located.

Acknowledgment

This work is supported by a grant from Natural Sciences and Engineering Research Council of Canada (NSERC).

References

- [1] S. Salvioli, E. Sikora, E.L. Cooper, C. Franceschi, Evid. Based Complement. Altern. Med. 4 (2007) 181–190.
- [2] R.K. Maheshwari, A.K. Singh, J. Gaddipati, R.C. Srimal, Life Sci. 78 (2006) 2081–2087.
- [3] Y.G. Lin, A.B. Kunnumakkara, A. Nair, W.M. Merritt, L.Y. Han, G.N. Rmaiz-Pena, A.A. Kamat, W.A. Spannuth, D.M. Gershenson, S.K. Lutgendorf, B.B. Aggarwal, A.K. Sood, Clin. Cancer Res. 13 (2007) 3423–3430.
- [4] A.B. Kunnumakkara, S. Guha, S. Krishnan, P. Diagaradjane, J. Gelovani, B.B. Aggarwal, Cancer Res. 67 (2007) 3853–3861.
- [5] Y.A. Mahmmod, Br. J. Pharmacol. 150 (2007) 200–208.
- [6] H. Nishino, A. Aoike, Cancer Res. 53 (1993) 1328–1331.
- [7] W. Win, Z. Cao, X. Peng, M.A. Trush, Y. Li, Mutat. Res. 513 (2002) 113–120.
- [8] A. Nedeljkovic, S. Radulovic, S. Bjeldglic, Arch. Oncol. 9 (2001) 171–174.
- [9] S. Usha, I.M. Johnson, R. Malathi, J. Biochem. Mol. Biol. 38 (2005) 198–205.
- [10] S. Usha, I.M. Johnson, R. Malathi, Mol. Cell Biochem. 284 (2006) 57–64.
- [11] J. Luo, T. Zhu, A. Evagelidis, M.D. Pato, J.W. Hanrahan, Am. J. Physiol. Cell Physiol. 279 (2000) C108–C119.
- [12] N.A. Kratochwil, W. Huber, F. Muller, M. Kansy, P.R. Gerber, Biochem. Pharmacol. 64 (2002) 1355–1374.
- [13] S. Sugio, A. Kashima, S. Mochizuki, M. Noda, K. Kobayashi, Protein Eng. 12 (1999) 439–446.
- [14] D.C. Carter, J.X. Ho, Adv. Protein Chem. 45 (1994) 153–203.
- [15] T. Peters, All about albumin. Biochemistry, Genetics and Medical Applications, Academic Press, San Diego, 1996.
- [16] X.M. He, D.C. Carter, Nature 358 (1992) 209–215.
- [17] T. Peters, Adv. Protein Chem. 37 (1985) 161–245.

- [18] S. Curry, P. Brick, N.P. Franks, *Biochim. Biophys. Acta* 1441 (1999) 131–140.
- [19] I. Petitpas, T. Grune, A.A. Battacharya, S. Curry, *J. Mol. Biol.* 314 (2001) 955–960.
- [20] E.L. Grelamo, C.H.T.P. Silva, H. Imasato, M. Tabak, *Biochim. Biophys. Acta* 1594 (2002) 84–99.
- [21] V.T.G. Chuang, M. Otagiri, *Biochim. Biophys. Acta* 1546 (2001) 337–345.
- [22] L. Painter, M.M. Harding, P.J. Beeby, *J. Chem. Soc., Perkin Trans. 18* (1998) 3041–3044.
- [23] S.Y. Lin, M.J. Li, Y.S. Wei, *Spectrochim. Acta Part A* 60 (2004) 3107–3111.
- [24] S. Krimm, J. Bandekar, *Adv. Protein Chem.* 38 (1986) 181–364.
- [25] R. Beauchemin, C.N. N'soukpoe-Kossi, T.J. Thomas, T. Thomas, R. Carpentier, H.A. Tajmir-Riahi, *Biomacromolecules* 8 (2007) 3177–3183.
- [26] D.M. Byler, H. Susi, *Biopolymers* 25 (1986) 469–487.
- [27] A. Ahmed, H.A. Tajmir-Riahi, R. Carpentier, *FEBS Lett.* 363 (1995) 65–68.
- [28] W.C. Johnson, *Proteins Struct. Funct. Genet.* 35 (1999) 307–312.
- [29] N. Sreerama, R.W. Woddy, *Anal. Biochem.* 287 (2000) 252–260.
- [30] T. Tang, S. Qi, X. Chen, *J. Mol. Struct.* 779 (2005) 87–95.
- [31] S. Bi, L. Ding, Y. Tian, D. Song, X. Zhou, X. Liu, H. Zhang, *J. Mol. Struct.* 703 (2005) 37–45.
- [32] W. He, Y. Li, C. Xue, Z. Hu, X. Chen, F. Sheng, *Bioorg. Med. Chem.* 13 (2005) 1837–1845.
- [33] C. Dufour, O. Dangles, *Biochim. Biophys. Acta* 1721 (2005) 164–173.
- [34] A. Ahmed Ouameur, S. Diamantoglou, M.R. Sedaghat-Herati, Sh. Nafisi, R. Carpentier, H.A. Tajmir-Riahi, *Cell Biochem. Biophys.* 45 (2006) 203–213.
- [35] L. Boulkanz, N. Balcarand, M.H. Baron, *Appl. Spectrosc.* 49 (1995) 1737–1746.
- [36] E. Bramanti, E. Benedetti, *Biopolymers* 38 (1996) 639–653.
- [37] J. Liu, J. Tian, Z. Hu, X. Chen, *Biopolymers* 73 (2004) 443–450.
- [38] M. Dockal, C. Chang, D.C. Carter, F. Ruker, *Protein Sci.* 9 (2000) 1455–1465.
- [39] E. Goormaghtigh, V. Cabiaux, J.M. Ruysschaert, *Eur. J. Biochem.* 193 (1990) 409–420.
- [40] J.R. Lakowicz, *Principles of Fluorescence Spectroscopy*, 2nd ed., Kluwer/Plenum, New York, 1999.
- [41] C.N. N'soukpoe-Kossi, M.R. Sedaghat-Herati, C. Ragi, S. Hotchandani, H.A. Tajmir-Riahi, *Int. J. Biol. Macromol.* 40 (2007) 484–490.
- [42] L. Liang, H.A. Tajmir-Riahi, M. Subirade, *Biomacromolecules* 9 (2008) 50–55.
- [43] A. Sulkowska, *J. Mol. Struct.* 614 (2000) 227–232.
- [44] U. Kragh-Hansen, *Dan. Med. Bull.* 37 (1990) 57–84.
- [45] F. Zsila, Z. Bikadi, M. Simonyi, *Tetrahedron Asymm.* 14 (2003) 2433–2444.
- [46] H.G. Mahesha, S. Singh, N. Srinivasan, A.G. Appu Rao, *FEBS J.* 273 (2005) 451–467.
- [47] L.D. Ward, *Methods Enzymol.* 117 (1985) 400–404.
- [48] B.X. Huang, C. Dass, Y.-H. Kim, *Biochem. J.* 387 (2005) 695–702.
- [49] M.R. Eftink, C.A. Ghiron, *Anal. Chem.* 114 (1981) 199–227.
- [50] C.Q. Jiang, M.X. Gao, J.X. He, *Anal. Chim. Acta* 452 (2002) 185–189.
- [51] M. Jiang, M.X. Xie, D. Zheng, Y. Liu, X.Y. Li, X. Chen, *J. Mol. Struct.* 692 (2004) 71–80.